

# We are IntechOpen, the world's leading publisher of Open Access books Built by scientists, for scientists

**4,800**

Open access books available

**122,000**

International authors and editors

**135M**

Downloads

Our authors are among the

**154**

Countries delivered to

**TOP 1%**

most cited scientists

**12.2%**

Contributors from top 500 universities



**WEB OF SCIENCE™**

Selection of our books indexed in the Book Citation Index  
in Web of Science™ Core Collection (BKCI)

Interested in publishing with us?  
Contact [book.department@intechopen.com](mailto:book.department@intechopen.com)

Numbers displayed above are based on latest data collected.

For more information visit [www.intechopen.com](http://www.intechopen.com)



## Chapter

# Study on Designing and Manufacturing a Radio-Frequency Generator Used in Drying Technology and Efficiency of a Radio Frequency-Assisted Heat Pump Dryer in Drying of *Ganoderma lucidum*

Nguyen Hay, Le Anh Duc and Pham Van Kien

## Abstract

A radio-frequency (RF) generator applied in drying technology was designed and manufactured for drying *Ganoderma lucidum*. The drying experiments were conducted by drying method of RF-assisted heat pump in order to inspect the operating parameters of the RF generator and investigate the effects of the input drying parameters on drying rate in the RF-assisted heat pump drying of *Ganoderma lucidum*. The results have shown that the RF generator achieved the required operating parameters as design such as RF power of 3 kW and operating frequency of 27 MHz. In RF-assisted heat pump drying, increase in RF power and drying air temperature increases the drying rate. Meanwhile, drying air velocity does not significantly affect the drying rate. At RF power of 1.95 kW, the drying time reduces by 9, 17, and 33% in comparison with RF power of 1.3, 0.65, and 0 kW (heat pump drying). At drying air temperature of 50°C, the drying time reduces by 10% and 21% in comparison with drying air temperature of 40 and 45°C. Besides, increasing RF power retains the higher content of polysaccharide in *Ganoderma lucidum*, and the *Ganoderma lucidum* samples retain the color better after drying.

**Keywords:** *Ganoderma lucidum*, heat pump, radio frequency, drying temperature, drying time

## 1. Introduction

Drying is a common and effective preservation technique that reduces moisture content of material to lower levels required. Therefore, drying can minimize the spoilage of various microbes in material and the physical, chemical, and biochemical changes within the drying products thereby increasing overall shelf life by considerable periods of time. However, the drying process will affect the quality of

the product such as nutritional standards, sensory standards, and physical and chemical standards. Therefore, the drying method and drying parameters should be considered to find a suitable drying method with optimum drying condition to retain a high quality of drying products, especially in food technology, agricultural products, and medicinal products.

*Ganoderma lucidum* is a medicinal product that contains various bioactive ingredients. Polysaccharide is a main bioactive ingredient in *Ganoderma lucidum* which has been found to be medically active in several therapeutic effects such as antitumor, anti-inflammatory, antiviral, anticancer, and anti-HIV [1]. However, polysaccharide and other bioactive ingredients in *Ganoderma lucidum* are heat sensitive and the high drying temperature tends to cause higher loss of active ingredients in dehydrated *Ganoderma lucidum*. Therefore, in drying *Ganoderma lucidum*, drying method as well as drying parameters should be considered carefully.

RF technology has shown some unique advantages in drying technology. RF heating is a volumetric heating method, which provides fast and deeper heat generation within material that increases heating rate and shortens drying time significantly. RF heating mechanism is described in **Figure 1**. In which, the RF generator creates an alternating electric field between two electrodes. The material is placed between the electrodes. The wet molecules within material continuously reorient themselves to face opposite poles of the alternating electric field. The friction resulting from the rotational movement of the molecules and the space-charge displacement causes the material to rapidly heat throughout its mass.

There were numerous studies of RF drying technology in which RF is combined with other drying methods as convection drying using hot air and freeze-drying for drying food and agricultural products [2–9]. The results show that heat generation within the whole volume of drying material that supports the heat transfer and moisture diffusion process to take place faster shortens the drying time and the temperature, and moisture distribution within material becomes more uniform. The drying products still retain their characteristic color and taste.

In heat pump drying with circulating drying air, drying air after being blown through the heat pump has the specific temperature, velocity, and humidity. Drying air will be blown into the drying chamber, and the drying process is performed here. In heat pump drying, the drying air temperature is at low level. So, the drying products can retain a high content of bioactive ingredients and their characteristic color and taste.

The drying technology using RF and heat pump drying has been found to be suitable for drying medicinal products. The objectives of this study are (1) to design

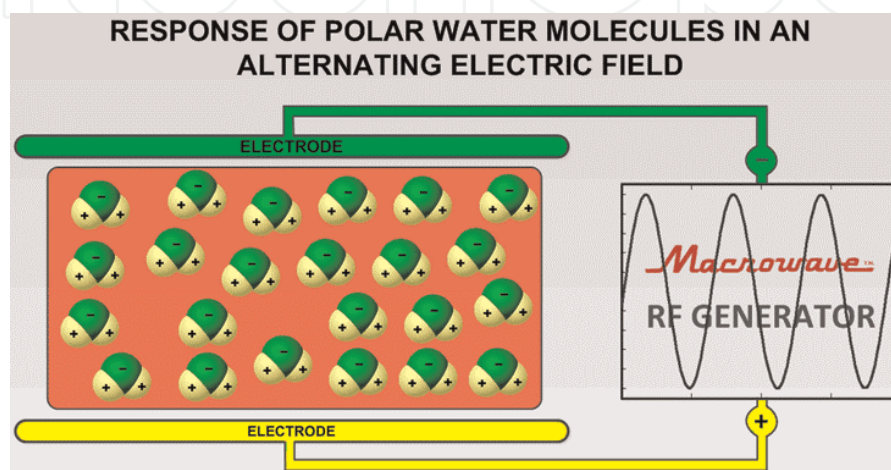


**Figure 1.**  
RF heating mechanism.

and manufacture a RF generator applied in drying technology for drying *Ganoderma lucidum*, in which RF-assisted heat pump drying method is applied, and (2) to investigate the effects of the input drying parameters as drying air temperature, drying air velocity and RF power on the drying rate, and the quality of *Ganoderma lucidum* in RF-assisted heat pump drying process.

## 2. Researching object and method

### 2.1 Researching object

A RF generator applied in drying technology is designed and manufactured in order to achieve a required maximum RF power of 3 kW and frequency of 27 MHz.

*Ganoderma lucidum* used for the experiments is red *Ganoderma lucidum* (*Ganoderma boninense*). After being harvested, *Ganoderma lucidum* has a moisture content of 3 (d.b) (i.e., 75% (w.b)), diameter of 12 cm, thickness of 1.5 cm, and glossy red brown color. *Ganoderma lucidum* samples are cleaned with dry tissues. The initial moisture content of the material is determined by a moisture analyzer (see **Table 1**).

### 2.2 Researching methods

#### 2.2.1 Designing and calculating method

- The required RF power is calculated based on physical and thermal properties of *Ganoderma lucidum* and theory of designing and calculating drying system.
- The circuit diagram and the components of the RF generator are designed and manufactured based on theory of RF heating mechanism, heat exchanger, and oscillator circuit of RF generator.

#### 2.2.2 Manufacture of RF generator method

The components of RF generator are manufactured in a single unit as designed and installed to complete a RF operator. Some standard components are selected and purchased in the market.

No	Symbol	Value
1	$G_b$	20 kg/batch
2	$m_{LC}$	20 kg
3	$\omega_i$	75% (w.b)
4	$\omega_f$	13% (w.b)
5	$C_p$	3.613 kJ/(kg °C)
6	r	3150 kJ/kg
7	$t_i$	30°C
8	$t_f$	45°C

**Table 1.**  
*Physical thermal index of the drying material.*

### 2.2.3 Measurement method

The parameters can be measured by specialized measuring instruments directly such as temperature, velocity of drying air, voltage, and electric current. The other parameters are determined by the exchange formulas.

### 2.2.4 Method of experiment

Experiments for investigation of the effects of the input drying parameters on drying rate in the RF-assisted heat pump drying of *Ganoderma lucidum* are conducted at the drying air temperature of 40, 45, and 50°C; drying air velocity of 1.2, 1.6, and 2.0 m/s; and RF power of 0.65, 1.3, and 1.95 kW.

### 2.2.5 Method of determining moisture content

The *Ganoderma lucidum* weight measurements are taken regularly after intervals of 20 minutes by an electronic scale digital balance (see **Table 1**). Each experiment is conducted until the drying material achieves the moisture content of 0.15 (d.b) (i.e., 13% (w.b)) and completed in triplicates.

The color of the drying products is measured by a colorimeter (see **Table 1**). The colorimeter displays three reflected light intensities corresponding to the lab color values. The total change in color of the drying *Ganoderma lucidum* sample with reference to the original sample is calculated as

$$\Delta E^* = \sqrt{(L_0 - L^*)^2 + (a_0 - a^*)^2 + (b_0 - b^*)^2} \quad (1)$$

The parameters in Eq. (1) are described in detail in part of 3.4.2 c. (3.4.2 c. Color of drying material).

Polysaccharide content of *Ganoderma lucidum* is determined by high-performance liquid chromatography (HPLC) method.

Statistical parameters such as mean and standard deviation are used to solve the experiment data. Examining the differences of the statistical data is conducted by means of least significant difference (LSD).

## 3. Results and discussions

### 3.1 The RF power of RF generator

The heat required for drying process was calculated based on the theory of calculating and designing drying system [10].

Physical and thermal property index of the drying material (*Ganoderma lucidum*) is given in **Table 2**.

#### 3.1.1 The heat required for heating the material

The heat required for heating the material in drying process is the heat of heating the drying material until the material achieves the required temperature. The required temperature of 45°C is chosen for calculation:

$$q_1 = m_{LC} \cdot C_p \cdot (t_f - t_i) = 20 \times 3.613 \times (45 - 30) = 1084 \text{ kJ} \quad (2)$$

The predictive time period required for *Ganoderma lucidum* to get the temperature of 45°C is 35 minutes. The heat required is calculated as

$$Q_1 = \frac{q_1}{\tau_1} = \frac{1084}{35 \times 60} = 0.516 \text{ kW} \quad (3)$$

### 3.1.2 The heat required for vaporizing water in the material

In the drying process, an amount of heat must be supplied to vaporize the water within drying material at specific drying temperature in order that the material achieves the required final moisture. The heat required depends on the mass of vaporized water in the material and latent heat of drying material.

The mass of vaporized water in the material (kg) is

$$G_W = \frac{m_{LC} \cdot (\omega_i - \omega_f)}{1 - \omega_f} = \frac{20 \cdot (0.75 - 0.13)}{1 - 0.13} = 14.25 \text{ kg} \quad (4)$$

So,

$$q_2 = G_W \cdot r = 14.25 \times 3150 = 44896 \text{ kJ} \quad (5)$$

The initial moisture content of *Ganoderma lucidum* is 75%. The predictive time period required for *Ganoderma lucidum* to get the final moisture content of 13% is 7 hours. The heat required is calculated as

$$Q_2 = \frac{q_2}{\tau_2} = \frac{44896}{7 \times 3600} = 1.782 \text{ kW} \quad (6)$$

No	Name	Description
1	Colorimeter	Type: Minolta CR-200
2	Frequency measurement instrument	Type: Acoustimeter CAT #A139 Max frequency: 70 ± 0.01 MHz
3	High-voltage voltmeter	Type: Voltmeter-MDP-50 K Voltage range resolution: 0.5–10 kVAC ±5%
4	Amperemeter	Type: Amperemeter-C.A401 Ampere range resolution: 0.1–10 A ± 1%
5	Thermal sensor	Type: AYN-MF59-104F-3950FB-1000 Measurement ranges: –60–300°C ± 0.05°C
6	Moisture analyzer	Type: DBS 60–3 model Maximum capacity: 60 g ± 0.01% Temperature range: 50–200°C Temperature increments: 1°C Repeatability (sd) with 2 g sample: 0.15% Moisture value predicted: 0–100%
7	Electronic scale digital balance	Type: DS-2002-N Max weighing capacity of 2000 ± 0.001 grams

**Table 2.**  
 Parameter index of the measurements.

### 3.1.3 The heat loss for heating the drying tray

In the drying process, the drying material is placed on a drying tray which is normally a plastic mesh grid. So, there must be an amount of heat loss for heating the drying tray until the drying tray gets the drying air temperature:

$$q_3 = m_{\text{tray}} \cdot C_{PVC} \cdot (t_f - t_i) = 25.05 \text{ kJ} \quad (7)$$

in which  $m_{\text{tray}}$  is the mass of the tray,  $m_{\text{tray}} = 1 \text{ kg}$ , and  $C_{P\_plastic}$  is the specific heat capacity of plastic,  $C_{P\_plastic} = 1.67 \text{ kJ}/(\text{kg } ^\circ\text{C})$ .

The predictive time period required for the drying tray to get the temperature of  $45^\circ\text{C}$  is 45 minutes. The heat loss is calculated as

$$Q_3 = \frac{q_3}{\tau_3} = \frac{25.05}{45 \times 60} = 0.009 \text{ kW} \quad (8)$$

### 3.1.4 Heat loss through pipes

In the drying process, the drying air flows inside a pipe system, and the outside wall of the pipe is in contact with environment. So, the heat loss through pipes should be considered, and it depends on the pipe material, size, length of the pipe, and drying temperature. The pipe is normally made of PVC plastic.

The length of pipe from the pump to the drying chamber is 1.5 m, so the surface area of the pipe is

$$S_0 = \pi \cdot d_2 \cdot l = 3.14 \times 0.2 \times 1.5 = 0.942 \text{ m}^2 \quad (9)$$

So, the heat loss through pipes is calculated as

$$Q_4 = S_0 \cdot q_4 = S_0 \cdot \lambda_{PVC} \cdot (t_f^v - t_i^v) \cdot \frac{2 \cdot \pi}{\ln \frac{d_2}{d_1}} = 0.374 \text{ kW} \quad (10)$$

in which  $t_i^v$  ( $30^\circ\text{C}$ ),  $t_f^v$  ( $45^\circ\text{C}$ ),  $d_1$  (0.193 m),  $d_2$  (0.2 m), and  $\lambda_{PVC}$  ( $\lambda_{PVC} = 0.15 \text{ W}/(\text{m } ^\circ\text{C})$ ) are temperature of the outside wall and inside wall, internal diameter, external diameter of the pipe, and thermal conductivity of PVC plastic.

### 3.1.5 Heat loss for heating the drying chamber

The drying process is performed in a drying chamber that is also heated up to the drying temperature. So, the heat loss for heating the drying chamber should be considered, and it depends on the material and mass of the chamber and drying temperature. In drying process of food and agricultural products, the drying chamber is normally made of a galvanized steel for food hygiene:

$$q_5 = m_{ch} \cdot C_{steel} \cdot (t_f^{ch} - t_i^{ch}) = 30 \times 0.49 \times (45 - 30) = 220.5 \text{ kJ} \quad (11)$$

The predictive time period required for the drying chamber to get the temperature of  $45^\circ\text{C}$  is 25 minutes. The heat loss is calculated as

$$Q_5 = \frac{q_5}{\tau_5} = \frac{220.5}{25 \times 60} = 0.147 \text{ kW} \quad (12)$$

in which  $m_{ch}$  (30 kg),  $t_1^{ch}$  (30°C), and  $t_2^{ch}$  (45°C) are mass of drying chamber, initial temperature, and final temperature of the drying chamber and  $C_{p\_steel}$  is specific heat of galvanized steel,  $C_{p\_steel} = 0.49 \text{ kJ}/(\text{kg } ^\circ\text{C})$ .

### 3.1.6 The heat loss through the drying chamber wall

The inside wall of drying chamber is in contact with drying air, and the outside wall is in contact with the environment. This causes the heat loss through the drying chamber wall in the drying process, and it depends on the material and area of the drying chamber. The area of the drying chamber ( $F$ ) includes the area of the drying chamber wall ( $F_w$ ) and two tops ( $F_t$ ).

The area of the drying chamber wall is

$$F_w = 2.(l_{ch}.h_{ch} + w_{ch}.h_{ch}) = 2 \times (1.25 \times 0.75 + 1.15 \times 0.75) = 3.6 \text{ m}^2 \quad (13)$$

After expanding the top of the drying chamber on computer by AutoCAD software, the surrounding area of a top is  $F_t = 1.62 \text{ m}^2$ .

So, the area of the drying chamber is

$$F = F_w + 2.F_t = 6,847 \text{ m}^2 \quad (14)$$

The heat loss is calculated as

$$Q_6 = q_5.F = k(t_{inside}^{ch} - t_{outside}^{ch}).F = 0.212 \text{ kW} \quad (15)$$

in which  $k$  is thermal conductivity of galvanized steel and  $k$  is  $2.06 \text{ W}/(\text{m}.\text{ }^\circ\text{C})$ .  $l_{ch}$ ,  $w_{ch}$ , and  $h_{ch}$  are the length, the width, and the height of the drying chamber.

### 3.1.7 Radiation heat loss

The radiation heat loss is calculated as

$$Q_7 = \varepsilon.F.C_0 \cdot \left[ \left( \frac{T_f}{100} \right)^4 - \left( \frac{T_i}{100} \right)^4 \right] = 0.593 \text{ kW} \quad (16)$$

in which  $\varepsilon$  is the radiation ratio of galvanized steel,  $\varepsilon = 0.85$ , and  $C_0$  is the radiation ratio of absolute black object,  $C_0 = 5.67 \text{ W}/(\text{m}^2.\text{K}^4)$ .

Thus, the total heat required for drying process is

$$Q_{total} = Q_1 + Q_2 + Q_3 + Q_4 + Q_5 + Q_6 + Q_7 = 3.632 \text{ kW} \quad (17)$$

In current study, the RF operator will be designed, manufactured, and applied in RF-assisted heat pump drying. So, in the drying process, RF heating has the main function of heating the material, vaporizing water within the material, and heating the drying tray. The other heat losses are supplied by heat pump. Thus, the heat required for RF generator is.

$$Q_{RF} = Q_1 + Q_2 + Q_3 = 2.307 \text{ kW} \quad (18)$$

Therefore, the RF power of RF generator is chosen  $P = 3 \text{ kW}$ .



### 3.2 Circuit diagram of RF generator

The circuit diagram of RF generator was designed based on the theory of RF heating mechanism, heat exchanger, and oscillator circuit of RF generator [11]. The circuit diagram of RF generator is described in **Figure 2**.

#### 3.2.1 Power supply unit

The power supply unit consists of a transformer, a wire supply voltage transformer, and a rectifier.

The transformer has the function of changing three-phase voltage 380 VAC into 6.5 kVAC. This high voltage is converted into DC voltage of 6.5 kVDC by the rectifier and supplied to the oscillation circuit. Besides, the wire supply voltage transformer will change the voltage from 380 VAC to 12.6 VAC to supply the triode tube filament.

#### 3.2.2 Oscillation circuit

The oscillation circuit consists of a high-frequency triode tube and LC oscillation circuits. A high voltage of 6.5 kVDC is applied to the anode of the triode tube after passing through an induction circuit including L1, L2, and C1 that acts as a filter circuit to remove the alternating current components of the supply power.

A high voltage of 12.6 VAC is applied to the filament and grid pin of the triode tube. A 12.6 VAC power is applied to the grid pin of the triode tube through an induction circuit that consists of L<sub>5</sub>, L<sub>6</sub>, and C<sub>4</sub>. The induction circuit controls the voltage of the grid pin to generate the output frequency at 27 MHz.

#### 3.2.3 RF emitting circuit

The RF emitting circuit is a circuit consisting of L<sub>3</sub> and C<sub>3</sub> in parallel. The RF high-frequency energy at the output of the high-frequency triode tube passes

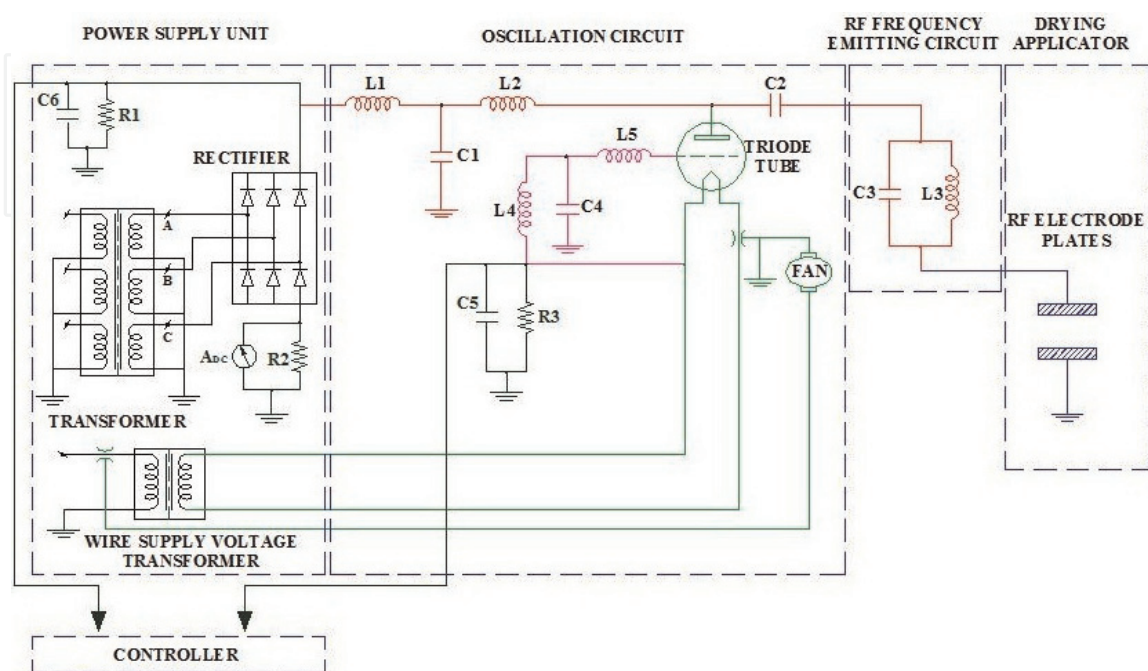


**Figure 2.**  
The circuit diagram of RF generator.

through the RF emitting circuit, and it is supplied to the electrode plates of the drying applicator.

### 3.2.4 Drying applicator

The drying applicator is composed of two parallel electrode plates which are called RF electrodes. The drying material is placed between the electrodes during drying process. The material is heated based on dielectric heating principle.

## 3.3 Fabricating the components of the RF generator

### 3.3.1 High-frequency triode tube

The high-frequency triode tube is selected in the market according to the required RF power, and it has the specific specifications as follows:

- Type: Toshiba 7T69RB.
- Voltage applied to filament: 12.6 VAC.
- Frequency: 27 MHz.
- Voltage applied to anode: 6.5 kVDC.
- Output power (maximum): 5 kW.

The output power of 5 kW will be converted to RF electrode plates in drying applicator at 60% efficiency (**Figure 3**).

### 3.3.2 Power supply unit

The transformers and the rectifier were manufactured at the workshop with the engineering specifications required. The transformer and rectifier are shown in **Figures 4** and **5**.



**High-frequency  
Triode tube**

**Figure 3.**  
*High-frequency triode tube.*

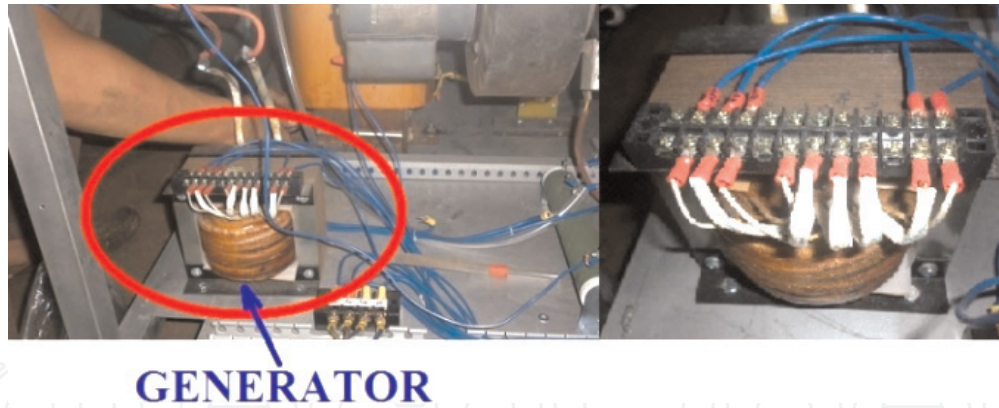


**Figure 4.**  
*Transformer.*

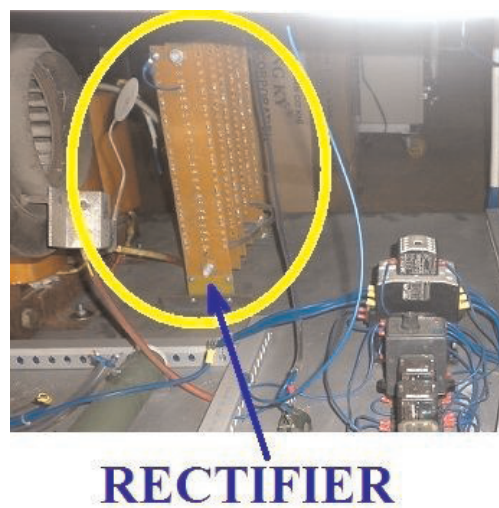


**Figure 5.**  
*Rectifier.*

### 3.3.3 Oscillation circuit

The oscillation circuit consists of numbers of capacitors and the inductor coils. The function of the oscillation circuit is amplifying the power and required generating frequency. The capacitors and the inductor coils are the industrial components that can work at the high voltage and high frequency (**Figure 6**).

The oscillation circuit consists of two induction circuits:

1. The  $L_1$ ,  $L_2$ , and  $C_1$  induction circuit works as a filter circuit to remove the alternating current components.
2. The  $L_4$ ,  $L_5$ , and  $C_4$  induction circuit regulates the voltage at the grid pin of the high-frequency triode tube to generate the output RF.

These capacitors and the inductor coils are selected and manufactured according to the standard in Strayfield's handbook for manufacturing RF generator [11], in which the capacitors  $C_1$  and  $C_4$  are selected in the market, while the inductors  $L_1$ ,  $L_2$ ,  $L_4$ , and  $L_5$  are manufactured at the workshop. Their values are as follows:

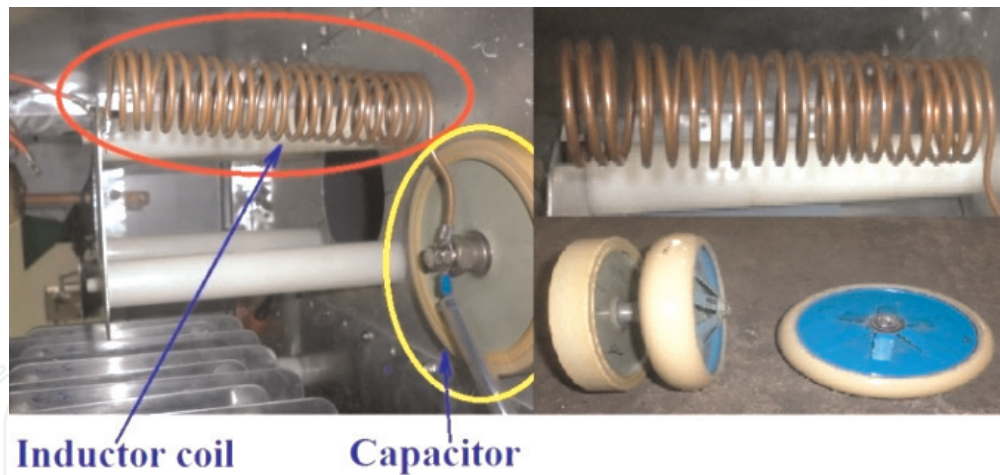


**Figure 6.**  
*Inductor coil and capacitor.*

$$C_1 = C_2 = 1500 \text{ pF}; C_4 = C_5 = C_6 = 500 \text{ pF}; L_1 = L_2 = L_4 = L_5 = 1.5 \times 10^{-6} \text{ H}.$$

### 3.3.4 RF emitting circuit

The structure of RF emitting circuit is composed of  $L_3$  and  $C_3$  in parallel that forms an induction circuit. The RF emitting circuit has the function of generating operating frequency of 27 MHz that is the technical requirements.  $L_3$  and  $C_3$  are manufactured in the workshop according to the technical requirements with the specifications below.

The structure of the capacitor  $C_3$  consists of two parallel electrode plates. The capacitance value of capacitor  $C_3$  depends on the area of the parallel electrode plates and distance between them.

The electrode plates have an area of  $A_{C_3} = 0.45 \times 0.45 = 0.203 \text{ m}^2$ , and the distance of two electrode plates is  $d_{C_3} = 0.1 \text{ m}$ .

The capacitance value of capacitor  $C_3$  is calculated as

$$C_3 = \frac{\epsilon_0 \cdot A_{C_3}}{4\pi \cdot k \cdot d_{C_3}} = 1.8 \times 10^{-11} \text{ F} \quad (19)$$

in which  $\epsilon_0$  ( $\epsilon_0 \approx 1$ ) is dielectric constant of air between two plates and  $k$  ( $k = 9 \times 10^9 \text{ N} \cdot \text{m}^2 / \text{C}^2$ ) is electrostatic constant.

The function of the  $L_3$  and  $C_3$  induction circuit is generating operating frequency of 27 MHz. So, the inductance value of  $L_3$  is calculated with the parameter  $f = 27 \text{ MHz}$  as follows:

$$L_3 = \frac{1}{(2\pi \cdot f)^2 \cdot C_3} = 1.9 \times 10^{-6} \text{ H} \quad (20)$$

The inductor  $L_3$  is manufactured in workshop with its specific specification as follows:

- Inductance value:  $L_3 = 1.9 \times 10^{-6} \text{ H}$ .
- Material: a copper wire.

- Diameter of wire: 2.5 mm.
- Diameter of wire coil: 40 mm.

### 3.3.5 Drying applicator

The drying applicator consists of two electrode plates which are called RF electrodes. The RF electrodes are fabricated at the workshop. The material used for fabrication of RF electrodes must be a good electric conductive material, and aluminum is chosen. The electrodes have a rectangular surface and dimension of 1200 mm × 1100 mm. They are fixed in drying chamber and connect to the RF emitting circuit through thin copper connectors. The distance between two electrodes is fixed by Teflon plastic bars. The RF electrodes are shown in **Figure 7**.

## 3.4 Drying experiment results

The RF-assisted heat pump dryer used in drying experiment is shown in **Figures 8** and **9**. In the drying process, the drying air is circulated over the evaporator of heat pump. The evaporator cools the drying air further down below the condensation temperature. Below this temperature, the drying air will be dehumidified. Then, the drying air is heated to the desired temperature inside the condenser and blown inside the drying chamber for drying process. In the drying chamber, the drying air will combine with the RF generated by the RF generator to conduct drying process of *Ganoderma lucidum*.

In drying experiment, the mass of *Ganoderma lucidum* selected is 4 kg. Thus, the RF power is adjusted to achieve the value of 0.65, 1.3, and 1.95 kW.

### 3.4.1 Result of operating parameters of RF generator

The RF generator is operated with the maximum RF power of 3 kW to inspect the operating parameters. The operating frequency of RF generator ( $f$ ) is measured by a frequency measurement instrument, the operating voltage ( $U$ ) is measured by a high-voltage voltmeter, and the operating current ( $I$ ) is measured by an amperemeter. The temperature of the material in drying process is measured by a thermal sensor that is connected to a computer through an integrated circuit. The temperature is recorded each 2 minutes.



**Figure 7.**  
*Electrode plates.*



The results show that the operation parameters achieve the designing requirement.

The engineering parameters of measurement instruments are described in the **Table 1**.

### 3.4.2 Evaluation of the effect of RF power

#### 3.4.2.1 Drying time

The drying curves of RF-assisted heat pump drying process at the drying air temperature of 45°C, drying air velocity of 1.2 m/s, and RF power of 0.65, 1.3, and 1.95 kW is presented graphically in **Figure 10**.

As shown in **Figure 10**, increasing RF power has a significant effect on moisture ratio; the moisture ratio is higher at higher RF power. At RF power of 1.95 kW, the drying time reduces by 9, 17, and 33% in comparison with RF power of 1.3, 0.65, and 0 kW (heat pump drying). It can be explained by RF heating mechanism, in which, increasing the RF power will increase energy absorption inside *Ganoderma lucidum*, which makes water dipole molecules and free ions in *Ganoderma lucidum*

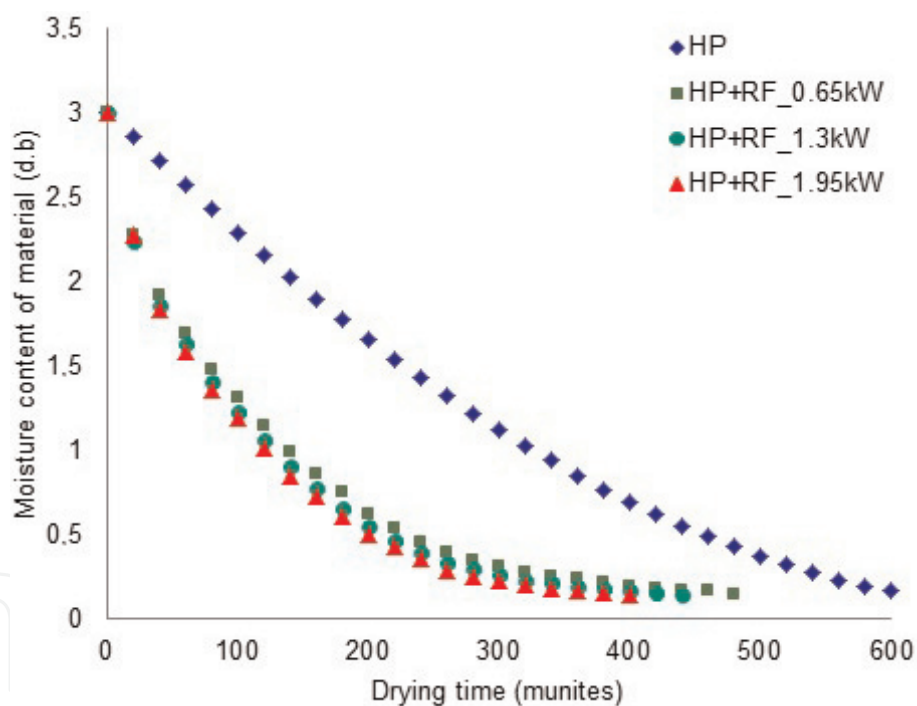


**Figure 10.**  
Drying curves of RF-assisted heat pump drying process at different RF powers.

No	Input drying parameter			Polysaccharide content (mg/g)
	$t_a$ (°C)	$v_a$ (m/s)	$P_{RF}$ (kW)	
1	45	1.2	0	7.82
2	45	1.2	0.65	9.18
3	45	1.2	1.3	9.31
4	45	1.2	1.95	9.47

**Table 3.**  
Polysaccharide content of *Ganoderma lucidum* after drying.

fluctuate faster. Thus, heat generation within *Ganoderma lucidum* becomes faster, and the moisture diffusion within *Ganoderma lucidum* occurs faster [12, 13].

#### 3.4.2.2 Polysaccharide content

The polysaccharide content of *Ganoderma lucidum* after drying is given in **Table 3**.

The data in **Table 3** shows that RF power has a significant effect on polysaccharide content of *Ganoderma lucidum* after drying. The polysaccharide content of *Ganoderma lucidum* after RF-assisted heat pump drying is considerably higher than heat pump drying. Increase in RF power retains the higher content of polysaccharide in *Ganoderma lucidum*. Generally, the reason for the degradation of polysaccharide content during drying of *Ganoderma lucidum* is due to hydrolysis, in which the polysaccharide is hydrolyzed as water is bound to the molecule [14]. RF-assisted heat pump drying process with RF heating mechanism shortens the heat treatment time, and an increase in RF power makes the linkage between water dipole molecules to be broken more easily. That can reduce the hydrolysis degree of polysaccharides.

#### 3.4.2.3 Color of drying material

Evaluation of the color change of *Ganoderma lucidum* before and after drying is conducted with X-Rite colorimeter following CIELAB scale. Fresh *Ganoderma lucidum* has the CIELAB original color value as  $L_0$ ,  $a_0$ , and  $b_0$ . *Ganoderma lucidum* after drying has the CIELAB color value as  $L^*$ ,  $a^*$ , and  $b^*$ . The color change index of *Ganoderma lucidum* corresponding to input drying parameters is shown in **Table 4**, in which the International Commission on Illumination (CIE) parameters as L, a, and b are measured with a colorimeter (see **Table 1**). The corresponding L value is lightness of color from 0 (black) to 100 (white); a value is degree of redness (0 to 60) or greenness (0 to -60); and b value is yellowness (0 to 60) or blueness (0 to -60). The total change in color ( $\Delta E^*$ ) of the drying *Ganoderma lucidum* sample with reference to the original sample is calculated as Eq. (1).

The data in **Table 4** shows that the color change index as  $\Delta L$ ,  $\Delta a$ , and  $\Delta b$  corresponding to RF-assisted heat pump drying is considerably smaller than

Type of sample	Color index						
	CIELAB color value			Color change index			
	$L_0$	$a_0$	$b_0$				
Fresh samples	47.12	4.11	18.85				
	$L^*$	$a^*$	$b^*$	$\Delta L$	$\Delta a$	$\Delta b$	$\Delta E^*$
Heat pump drying ( $P_{RF} = 0$ kW)	36.5 <sup>a</sup>	6.94 <sup>a</sup>	12.52 <sup>a</sup>	10.62	2.83	6.33	12.68 <sup>a</sup>
RF-assisted heat pump drying ( $P_{RF} = 0.65$ kW)	38.71 <sup>b</sup>	5.75 <sup>b</sup>	13.76 <sup>b</sup>	8.41	1.64	5.09	9.97 <sup>b</sup>
RF-assisted heat pump drying ( $P_{RF} = 1.3$ kW)	39.02 <sup>c</sup>	5.42 <sup>c</sup>	14.1 <sup>c</sup>	8.1	1.31	4.75	9.48 <sup>c</sup>
RF-assisted heat pump drying ( $P_{RF} = 1.95$ kW)	39.35 <sup>d</sup>	5.12 <sup>d</sup>	14.46 <sup>d</sup>	7.77	1.01	4.39	8.98 <sup>d</sup>

Mean values in the same column with different letter symbols. Significant difference at significance level of 0.05.

**Table 4.**  
 The CIELAB color values of *Ganoderma lucidum*.



heat pump drying and increase in RF power decreases the color change index values. Thus, the *Ganoderma lucidum* samples have retained the color better at higher RF power and at RF power of 1.95 kW, and the color of *Ganoderma lucidum* samples is nearly similar to the original brown red of fresh material samples.

### 3.4.3 Evaluation of the effect of drying air temperature

The drying curves of RF-assisted heat pump drying process at the drying air temperature of 40, 45, and 50°C, drying air velocity of 1.2 m/s, and RF power of 1.3 kW is presented graphically in **Figure 11**.

As shown in **Figure 11**, increasing drying air temperature has a significant effect on moisture ratio; the moisture ratio is higher at higher drying air temperature. At drying air temperature of 50°C, the drying time reduces by 10% and 21% in comparison with drying air temperature of 40 and 45°C. It can be explained by the fact that the increase in drying air temperature will increase the amount of heat absorbed by material. Thus, the heating rate increases, and the moisture diffusion within *Ganoderma lucidum* occurs faster.

### 3.4.4 Evaluation of the effect of drying air velocity

The drying curves of RF-assisted heat pump drying process at the drying air temperature of 45°C; drying air velocity of 1.2, 1.6, and 2 m/s; and RF power of 1.3 kW is presented graphically in **Figure 12**.

As shown in **Figure 12**, increasing drying air velocity makes drying time become longer. This is explained by the fact that the increase in drying air velocity will increase the drying airflow in contact with the drying material surfaces. The

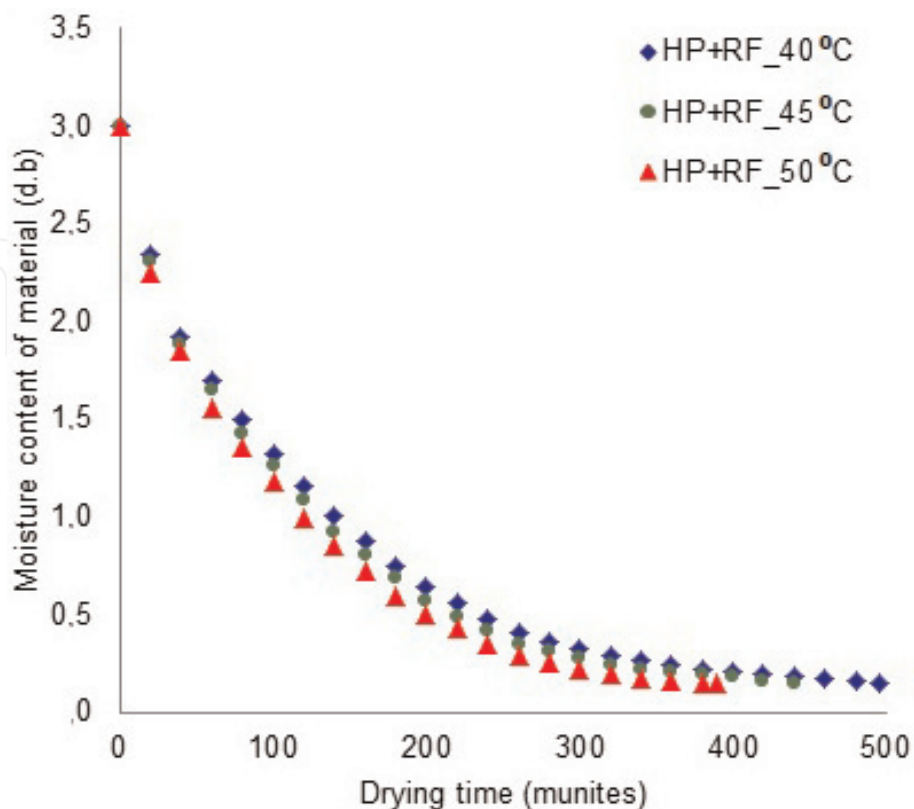


**Figure 11.** Drying curves of RF-assisted heat pump drying process at different drying air temperatures.

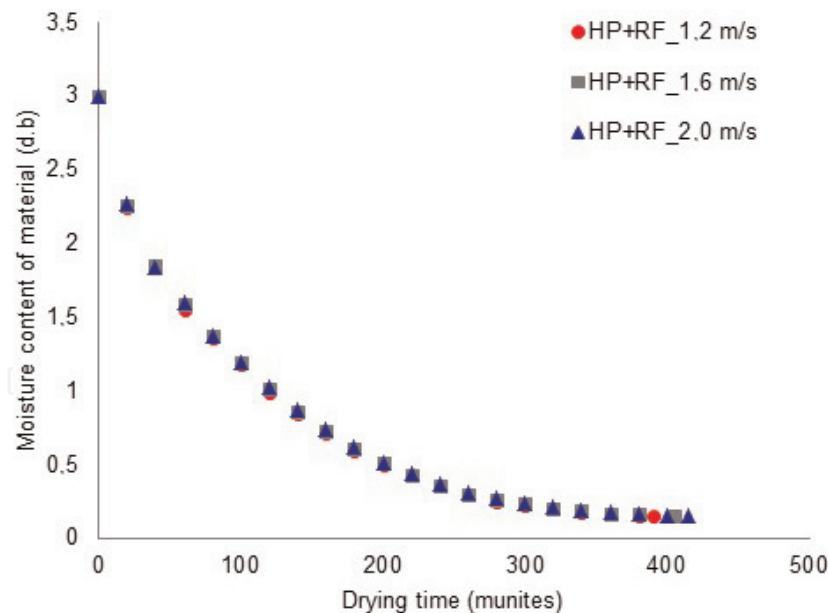


**Figure 12.**  
 Drying curves of RF-assisted heat pump drying process at different drying air velocities.

temperature of drying material is maintained at a higher level than drying air temperature during drying process by RF heating mechanism. So, when drying air comes into contact with drying material surfaces, the temperature of material surfaces will decrease that causes the average temperature of material to decrease and drying time to become longer. However, drying air velocity does not significantly affect the drying rate. The drying time corresponding to three drying air velocity values differs only about 10–15 minutes, and the drying curves shown in **Figure 12** are almost identical. The experimental results are in agreement with the previous studies of agricultural product drying [15–18].

#### 4. Conclusions

Based on the calculation and design results, the RF generator has been successfully manufactured and applied in drying technology. The RF generator worked efficiently and achieved the required RF power of 3 kW and frequency of 27 MHz as designed. The drying experiment results showed that in RF-assisted heat pump drying, increase in RF power and drying air temperature increases the drying rate considerably. Meanwhile, drying air velocity does not significantly affect the drying rate. Besides, when RF power increases, the *Ganoderma lucidum* samples retain the higher content of polysaccharide and the original color better after drying.

#### Nomenclature

AC	alternating current
C	capacitor
$C_p$	specific heat of drying material, J/(kg °C)
d.b	dry basic (kg H <sub>2</sub> O/kg dry solid)
DC	direct current
f	frequency, MHz
$G_b$	drying capacity, kg/batch
h	the height, m

HP	heat pump
HPLC	high-performance liquid chromatography
I	ampere, A
l	the length, m
L	inductor coil
LSD	least significant difference
$m_{LC}$	mass of <i>Ganoderma lucidum</i> , kg
M	moisture of drying material, d.b
$P_{RF}$	RF power, kW
Q	the heat, kW
r	latent heat of vaporization of moisture in material, J/kg
RF	radio frequency
t	temperature of drying material, °C
T	absolute temperature of drying material, °K
U	voltage, kV
w	the width, m
w.b	wet basic (kg H <sub>2</sub> O/kg wet solid)

### Greek symbols

$\lambda$	thermal conductivity, W/m °C
$\omega$	moisture of drying material, w.b
$\varepsilon$	radiation ratio of galvanized steel
$\tau$	the time, s

### Subscripts

i	initial
f	final
W	water
ch	chamber

### Author details

Nguyen Hay<sup>1\*</sup>, Le Anh Duc<sup>1\*</sup> and Pham Van Kien<sup>2</sup>


1 Nong Lam University, Ho Chi Minh City, Vietnam

2 LILAMA2 International Technology College, Dong Nai, Vietnam

\*Address all correspondence to:

ng.hay@hcmuaf.edu.vn and leanhduc@hcmuaf.edu.vn

### IntechOpen

© 2019 The Author(s). Licensee IntechOpen. This chapter is distributed under the terms of the Creative Commons Attribution License (<http://creativecommons.org/licenses/by/3.0>), which permits unrestricted use, distribution, and reproduction in any medium, provided the original work is properly cited. 

## References

- [1] Perumal K. Indigenous Technology on Organic Cultivation of Reishi (*Ganoderma lucidum*). Taramani, Chennai: Shri AMM Murugappa Chettiar Research Centre; 2009
- [2] Ptasznik W, Zygmunt S, Kudra T. Simulation of RF assisted convective drying for seed quality broad bean. *Drying Technology*. 1990;**8**:977-992
- [3] Jumah R. Modelling and simulation of continuous and intermittent radio frequency assisted fluidized bed drying of grains. *Food and Bioproducts Processing*. 2005;**83**:203-210
- [4] Yanhong L et al. Heating patterns of white bread loaf in combined radio frequency and hot air treatment. *Journal of Food Engineering*. 2013;**116**:472-477
- [5] Kaya A. Numerical analysis of a radio frequency assisted convective drying. *International Journal of Scientific & Technology Research*. 2015;**4**:234-241
- [6] Huang Z, Zhu H, Yan R, Wang S. Simulation and prediction of radio frequency heating in dry soybeans. *Biosystems Engineering*. 2015;**129**:34-47
- [7] Houa L, Huang Z, Koua X, Wang S. Computer simulation model development and validation of radio frequency heating for bulk chestnuts based on single particle approach. *Food and Bioproducts Processing*. 2016;**100**:372-381
- [8] Jiao S, Zhu D, Deng Y, Zhao Y. Effects of hot air assisted radio frequency heating on quality and shelf-life of roasted peanuts. *Food and Bioprocess Technology*. 2016;**9**:308-319
- [9] Zhu H, Li D, Shujun L, Wang S. A novel method to improve heating uniformity in mid-high moisture potato starch with radio frequency assisted treatment. *Journal of Food Engineering*. 2017;**206**:23-36
- [10] Van Phu T. Calculating and Designing Drying System. Ha Noi, Vietnam: Education Publisher; 2002. p. 360
- [11] Arun M. Radio frequency drying systems for the textile. In: *Industry Handbook*. England: Strayfield Limited; 2007. p. 352
- [12] Houa L, Linga B, Wang S. Development of thermal treatment protocol for disinfesting chestnuts using radio frequency energy. *Postharvest Biology and Technology*. 2016;**98**:65-71
- [13] Ozturk S, Kong F, Singh RK, Kuzy JD, Li C. Radio frequency heating of corn flour: Heating rate and uniform. *Innovative Food Science & Emerging Technologies*. 2017;**171**:234-241
- [14] Chin SK, Law CL, Cheng PG. Effect of drying on crude ganoderic acids and water soluble polysaccharides content in *Ganoderma lucidum*. *International Journal of Pharmacy and Pharmaceutical Sciences*. 2011;**3**:38-43
- [15] Celma AR, Cuadros F, Lopez-Rodriguez F. Review: Characterization of industrial tomato by products from infrared drying process. *Food and Bioproducts Processing*. 2009;**87**:282-291
- [16] Younis M, Abdelkarim D, El-Abdein AZ. Kinetics and mathematical modeling of infrared thin—Layer drying of garlic slices. *Saudi Journal of Biological Sciences*. 2017;**80**:25-32
- [17] Sharma GP, Prasad S, Chahara VK. Moisture transport in garlic cloves undergoing microwave—Convective drying. *Food and Bioproducts Processing*. 2009;**87**:11-16
- [18] Duc LA, Han J-W. The effects of drying conditions on the germination properties of rapeseed. *Journal of Biosystems Engineering*. 2009;**34**:30-36